Do High-Spin Topology Rules Apply to Charged Polyradicals? Theoretical and Experimental Evaluation of Pyridiniums as Magnetic Coupling Units

Anthony P. West, Jr., Scott K. Silverman, and Dennis A. Dougherty*

Contribution No. 9118 from the Arnold and Mabel Beckman Laboratories of Chemical Synthesis, Division of Chemistry and Chemical Engineering, California Institute of Technology, Pasadena, California 91125

Received August 14, 1995[⊗]

Abstract: *Ab initio* calculations on pyridine and pyridinium analogues of *m*-xylylene indicate that the neutral heterocycle is essentially equivalent to benzene as a ferromagnetic coupling unit, while the cationic pyridiniums behave much differently. Depending on the substitution pattern, a protonated pyridine can serve as a ferromagnetic coupling unit or an antiferromagnetic coupling unit. Both valence bond and molecular orbital arguments provide qualitative rationalizations of these results. In an effort to test the theoretical predictions, bis(trimethylenemethane) analogues of the pyridine and pyridinium biradicals were synthesized and analyzed by electron paramagnetic resonance spectroscopy. General support for the theoretical predictions is obtained.

Introduction

Over the last 20 years, great advances have been made in our understanding of the spin-state preferences of organic molecules with two or more unpaired electrons.[1] A number of biradical systems have been characterized, and well-understood theoretical models allow predictions concerning new systems.[2,3] The coupling rules for biradicals can be rationally extended to polyradicals, allowing the design of very high-spin organic molecules.

Certainly the best studied, most reliable high-spin coupling strategy has been "meta through a benzene". The prototype is the biradical *m*-xylylene (**1**), which exhibits a substantial preference for the triplet ground state.[4] The simple methylene radicals ($CH_2^{\bullet}$) of *m*-xylylene can be replaced by a wide array of spin-containing structures, and high-spin ground states are invariably produced. This has led to the notion of *m*-phenylene as a general ferromagnetic coupling unit. The origin of this high-spin preference is well understood and can be expressed in terms of several different models. Fundamentally, the *topology* of the *m*-xylylene π-system is crucial. Throughout this work, we use the word "topology" to denote the connectivity of the molecules rather than any properties of the molecular orbitals. A simple statement of the role of topology in determining the spin preferences of planar π-systems is the */non-* rule. In alternant π-systems the atoms can be divided into two sets, * and non-*, such that no two members of the same set are connected. If, as in *m*-xylylene, the * set outnumbers the non-* by 2 (see **1a**), a triplet ground state is generally expected, and spin density will reside only on the starred atoms.[5]

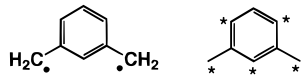

1 **1a**

It has been explicitly predicted that this topological rule will hold even if heteroatoms are incorporated into the system.[2b] For

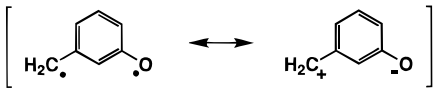

2

example, consider *m*-quinomethane (**2**).[6] This biradical has a triplet (**T**) ground state, and theoretical studies[6b] as well as recent experimental data on a related system[7] indicate that the magnitude of the preference is quite substantial. This occurs despite the zwitterionic resonance structure shown, which must preferentially stabilize the *singlet* state. It is well known that ionic terms in a wave function preferentially stabilize singlet states. Given the availability of a very attractive zwitterionic form for *m*-quinomethane, which is much less attractive in *m*-xylylene, one might have expected a smaller **S**−**T** gap in the former, and perhaps even a **S** ground state. But this is not the case: topology wins out. The more drastic effect of introducing a charge into a high-spin system and the extent to which topology rules are then applicable have been little studied. A notable exception, however, is the important series of

[⊗] Abstract published in *Advance ACS Abstracts,* January 15, 1996.

(1) Dougherty, D. A. *Acc. Chem. Res.* **1991**, *23*, 88−94. Iwamura, H.; Koga, N. *Acc. Chem. Res.* **1993**, *26*, 346−351. Rajca, A. *Chem. Rev.* **1994**, *94*, 871−893. Borden, W. T.; Iwamura, H.; Berson, J. A. *Acc. Chem. Res.* **1994**, *27*, 109−116.

(2) (a) Borden, W. T.; Davidson, E. R. *J. Am. Chem. Soc.* **1977**, *99*, 4587−4594. (b) Ovchinnikov, A. A. *Theor. Chim. Acta* **1978**, *47*, 297−304.

(3) Note that, in general, theoretical predictions of high-spin ground states are more reliable than predictions of low-spin ground states.

(4) Kato, S.; Morokuma, K.; Feller, D.; Davidson, E. R.; Borden, W. T. *J. Am. Chem. Soc.* **1983**, *105*, 1791−1795. Fort, R. C., Jr.; Getty, S. J.; Hrovat, D. A.; Lahti, P. M.; Borden, W. T. *J. Am. Chem. Soc.* **1992**, *114*, 7549−7552.

(5) There are hydrocarbon exceptions to this rule that are well-understood and can be anticipated (see ref 2a). Note also, that generally, there is negative spin density on the non-* atoms.

(6) (a) Rule, M.; Matlin, A. R.; Hilinski, E. F.; Dougherty, D. A.; Berson, J. A. *J. Am. Chem. Soc.* **1979**, *101*, 5098−5099. Rule, M.; Matlin, A. R.; Seeger, D. E.; Hilinski, E. F.; Dougherty, D. A.; Berson, J. A. *Tetrahedron* **1982**, *38*, 787−798. (b) Lahti, P. M.; Ichimura, A. S.; Berson, J. A. *J. Org. Chem.* **1989**, *54*, 958−965.

(7) Khan, M. I.; Goodman, J. L. *J. Am. Chem. Soc.* **1994**, *116*, 10342−10343.

0002-7863/96/1518-1452$12.00/0

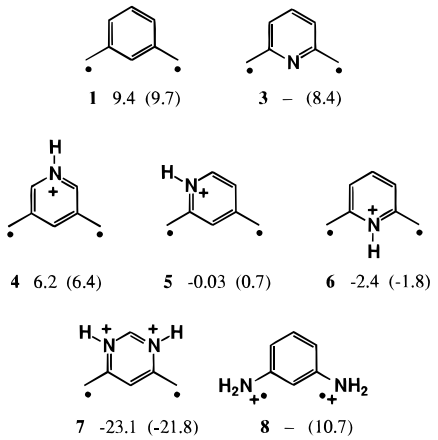

Figure 1. Calculated 6-31G* (6-31G) π-CISD singlet−triplet gaps of **1** and **3**−**8**. Positive values indicate a triplet ground state.

investigations of the radical anion and radical cation of the prototype high-spin biscarbene *m*-phenylenebis(phenylmethylene).[11]

We describe here the first examples of *planar* molecules with *m*-xylylene topologies but *singlet* ground states.[8,9] Replacement of the benzene ring of **1** with pyridine (e.g., **3**) produces a minimal perturbation of the **S**−**T** gap,[10] consistent with the previous prediction concerning heteroatoms. However, conversion to a pyridinium as in **4**−**6** has profound effects on **S**−**T** gaps.

In the current work, the primary evidence is computational, using high-level *ab initio* calculations of a type that have been reliable in related systems.[4] The theory makes a number of clear-cut predictions, including several violations of the topology (i.e., */non-*) rules. We have also made a considerable effort to experimentally test the theoretical predictions. The experimental results generally support the theory, and suggest the potential for novel magnetic coupling mechanisms in pyridinium structures.

Computational Results

Our targets have been structures related to *m*-xylylene (**1**), in which the central benzene ring is replaced by a pyridine or pyridinium ring. The results are summarized in Figure 1. Briefly, the methodology involves full geometry optimization (planarity enforced) for both the singlet and triplet states, using GVB (two-configuration SCF) and UHF wave functions, respectively. Correlation effects were examined a number of ways including configuration interaction with all single and double excitations in the full π-space. None of the basic conclusions we will reach are especially sensitive to the level of theory (see the Experimental Section).

Substitution of a pyridine for a benzene as in **3** has very little effect on the **S**−**T** gap. This finding is certainly not surprising, given the results for *m*-quinomethane. However, substituting a pyridinium ring into the *m*-xylylene topology substantially influences **S**−**T** gaps. Importantly, this is not a generic coulombic or electrostatic effect, since it is quite sensitive to the position of the charge. The π-topologies of structures **1**−**8** are identical, but major changes in **S**−**T** gaps are seen.

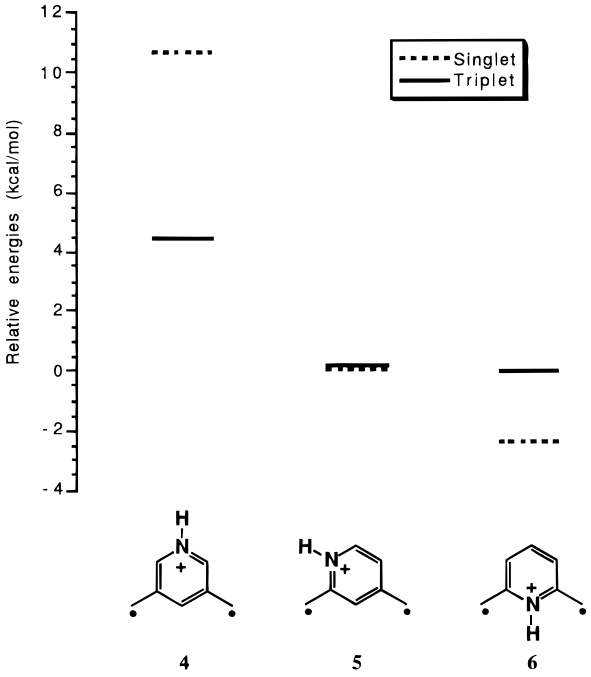

Figure 2. Relative energies (6-31G* π-CISD) of the singlet and triplet states of the three isomers **4**, **5**, and **6**. The triplet state of **6** was taken as the zero of energy.

In **4**, there is still a large preference for a **T** ground state. It is perhaps slightly diminished relative to **1**, but this is not of central importance here. Note that in **4** the perturbation is introduced at a non-* position, where, to first order, there is no spin density. Thus, it is not surprising that no major change in electronic structure is seen.

In both **5** and **6** the NH^+ is at an active (*) site, and a significant perturbation seems possible. In **5**, **S** and **T** are best thought of as essentially degenerate at this level of theory. The deviation of the **S**−**T** gap from zero is small, and its sign depends on the level of theory. For **6**, however, all levels of theory considered here predict **S** < **T**. While the gap is not large in magnitude, its persistence across several levels of theory and the previous successes of the highest levels used here[4] lead us to conclude that in the gas phase, biradical **6** has a singlet ground state. Thus, planar 2,6-pyridiniumdiyl is a weak antiferromagnetic coupling unit.

To further probe the role of charge in influencing **S**−**T** gaps, we evaluated the dications **7** and **8**, with dramatically different results. Structure **7** is now unambiguously a singlet ground state. We doubt that such a large **S**−**T** gap could be reversed by any higher level of theory. In sharp contrast, the isomeric dication **8** shows a triplet ground state, with a **S**−**T** gap similar to the parent hydrocarbon **1**.[12]

One can develop several models to explain the results of Figure 1. Since **4**−**6** are isomers, their six spin states can all be put on the same energy scale, and this is done in Figure 2. It can be seen that the *singlet* states of the biradicals are much more sensitive to the position of the charge. To a good approximation, the progression **4** → **5** → **6** represents a

(8) There are some other topologies for which true violations of the */non-* rule arise due to heteroatom substitutions. See: Du, P.; Hrovat, D. A.; Borden, W. T. *J. Am. Chem. Soc.* **1989**, *111*, 3773−3778.

(9) *Nonplanar* analogues of **1** can be low spin. See: Dvolaitzky, M.; Chiarelli, R.; Rassat, A. *Angew. Chem., Int. Ed. Engl.* **1992**, *31*, 180−181. Kanno, F.; Inoue, K.; Koga, N.; Iwamura, H. *J. Am. Chem. Soc.* **1993**, *115*, 847−850.

(10) Preliminary results on a neutral pyridine structure (**12**) have been reported: Dougherty, D. A.; Jacobs, S. J.; Silverman, S. K.; Murray, M.; Shultz, D. A.; West, A. P., Jr.; Clites, J. A. *Mol. Cryst. Liq. Cryst.* **1993**, *232*, 289−304. See also: Chaler, R.; Carilla, J.; Brillas, E.; Labarta, A.; Fajari, L.; Riera, J.; Juliá, L. *J. Org. Chem.* **1994**, *59*, 4107−4113.

(11) Matsushita, M.; Nakamura, T.; Momose, T.; Shida, T.; Teki, Y.; Takui, T.; Kinosha, T.; Itoh, K. *J. Am. Chem. Soc.* **1992**, *114*, 7470−7475. Matsushita, M.; Nakamura, T.; Momose, T.; Shida, T.; Teki, Y.; Takui, T.; Kinosha, T.; Itoh, K. *Bull. Chem. Soc. Jpn.* **1993**, *66*, 1333−1342.

(12) For experimental studies of a related system, see: Stickley, K. R.; Blackstock, S. C. *J. Am. Chem. Soc.* **1994**, *116*, 11576−11577.

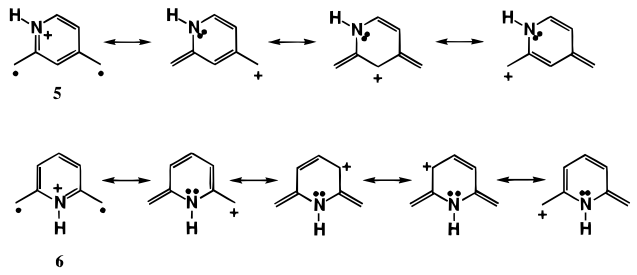

Figure 3. Resonance structures for **5** and **6**.

continuing, preferential stabilization of the singlet relative to the triplet. As is generally the case with biradical systems, both valence bond (VB) and molecular orbital (MO) arguments can be developed, and we will present both below.

The VB arguments emphasize resonance structures (Figure 3). The key is that the singlet states benefit from *closed-shell* resonance structures, as well as biradical resonance structures, while the triplets can utilize only biradical-type resonance structures. Given this, the trend across the **4**−**6** series can be understood.

For **4**, there are no favorable closed-shell resonance structures available. So, it behaves like a simple, *m*-xylylene, and **T** lies below **S** by a substantial margin. For **5**, however, several closed-shell singlet resonance structures are accessible (Figure 3). These greatly stabilize the singlet, and indeed, the biggest difference between **4** and **5** is the much greater stability of ^{1}**5** relative to ^{1}**4**. There is also some independent stabilization of ^{3}**5**, and the net effect is that, coincidentally, ^{1}**5** and ^{3}**5** are nearly degenerate.

In ^{1}**6**, there is an additional closed-shell resonance structure relative to ^{1}**5** (Figure 3), and the major difference between **6** and **5** is the preferential stabilization of ^{1}**6**: the two triplet states are essentially degenerate (Figure 2). Basically, the difference between ^{1}**6** and ^{1}**5** is that the former contains a heptatrienyl cation, while the latter contains a pentadienyl cation with a cross-conjugated vinyl group.

For both the singlet and the triplet of a hydrocarbon biradical such as **1**, VB arguments typically consider only *covalent* states—those in which each p orbital is occupied by exactly one electron. There are also singlet (but not triplet) *ionic* states in which some p orbitals are doubly occupied or empty, but these are usually much too high in energy to be significant. Clearly, though, many of the resonance structures of Figure 3 would be associated with *ionic* states. Since these resonance structures are much more stable than analogous structures that would be written for **1**, the conventional ionic states of **5** and **6** are much lower in energy. Their stabilizing contribution to the lowest singlet state is correspondingly larger, and so the **S**−**T** gap is diminished (**5**) and ultimately reversed (**6**).

Evidence that this resonance model is sound can be found by examining the calculated geometries of **6** (Figure 4). Compared to appropriate reference structures, the exocyclic C−C bonds of ^{1}**6** are significantly shortened, consistent with the double bond character expected from resonance.

Arguments based on MO theory emphasize the role of the nonbonding MOs (NBMOs). The Hückel NBMOs of **1** are sketched in Figure 5. At high levels of theory, they are not strictly degenerate, but they are very nearly so. In addition, the topology of the π-system dictates that the NBMOs are nondisjoint, producing destabilizing exchange repulsions in the singlet state and thus a triplet ground state.[2] Opening up an energy gap between the NBMOs favors closed-shell structures and hence singlet ground states. On substituting a CH by an NH^+, one is introducing a much more electronegative group,

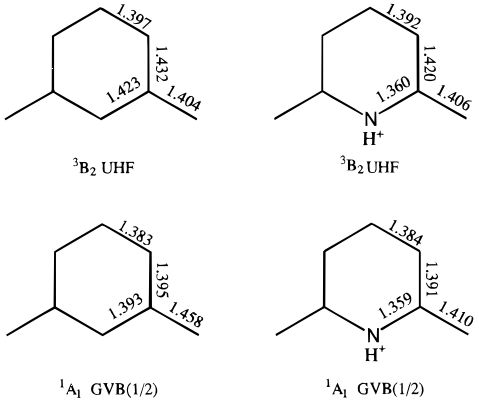

Figure 4. Geometries of the singlet and triplet states of **1** and **6**, showing bond lengths in angstroms.

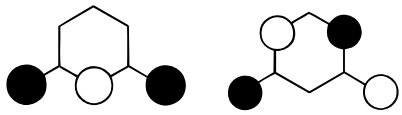

Figure 5. Hückel nonbonding molecular orbitals of **1**.

and this should stabilize an MO roughly in proportion to the coefficient at the NH^+ center. One can develop a qualitative understanding of our results based on such reasoning.

In **4**, the NH^+ is introduced at a position where there are negligible coefficients in both NBMOs. Hence, very little perturbation occurs, and **4** behaves like **1**. In both **5** and **6**, however, the NH^+ is introduced at a site that has a large coefficient in one NBMO, and a negligible coefficient in the other. This preferentially stabilizes one NBMO relative to the other, opens up a HOMO−LUMO gap, and preferentially stabilizes the closed-shell **S** state. It is tempting to conclude that ^{1}**6** is more stable than ^{1}**5** because of the larger NBMO coefficient at the perturbed center (0.57 vs 0.50 in the canonical Hückel orbitals of **1**), but this may be pushing such qualitative arguments too far.

These MO arguments led us to consider the extreme case of **7**. Now, one NBMO is doubly perturbed, while the other is, to first order, unchanged. This should open up a very large HOMO−LUMO gap, and indeed, a very large preference, **S** < **T**, is seen (Figure 1). Conversely, the double perturbation in **8** should affect both NBMOs, and no strong effect on the **S**−**T** gap is observed.

Experimental Tests of Theoretical Predictions

One can envision a number of approaches to experimentally test the above predictions. In principle, direct characterization of the biradicals **3**−**6** might be feasible, although they represent a substantial synthetic challenge. Alternatively, one could prepare biscarbene analogues of **3**−**6**, as polycarbenes have certainly been the most successful tool for evaluating the spin topology rules. The key, of course, is to develop a protocol for protonating the pyridine ring of an appropriate precursor, without degrading the precursor. While synthesis of the biradicals or biscarbenes might be feasible, we have adopted an alternative strategy.

Recently, we have shown that the bis(trimethylenemethane) [bis(TMM)] strategy is useful for evaluating potential ferromagnetic and antiferromagnetic coupling units.[13,14] In this approach, one replaces the radical centers of the biradical of

(13) Jacobs, S. J.; Shultz, D. A.; Jain, R.; Novak, J.; Dougherty, D. A. *J. Am. Chem. Soc.* **1993**, *115*, 1744−1753.
(14) Silverman, S. K.; Dougherty, D. A. *J. Phys. Chem.* **1993**, *97*, 13273−13283.

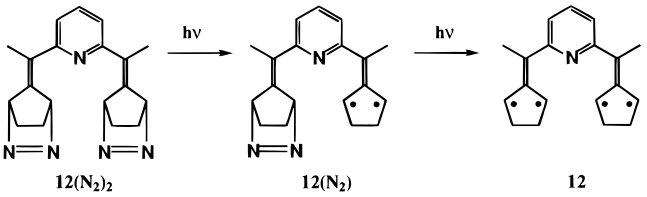

Figure 6. Standard photolysis sequence for the bis(TMM) strategy.

interest with 2-alkylidene-1,3-cyclopentanediyls, derivatives of the prototype triplet biradical trimethylenemethane. Ferromagnetic coupling of two triplet TMMs produces a quintet (**Q**) tetraradical. Alternatively, if two TMMs are linked through a structure that is not a strong ferromagnetic coupling unit, triplet or singlet states might be expected for the resulting tetraradical.

For example, the bis(TMM) analogue of **1** is tetraradical **9**. We have shown that **9** has a quintet ground state, with no detectable thermal population of lower spin states at temperatures as high as 135 K. In addition, we have extensively

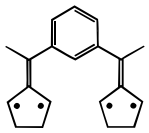

9

developed the electron paramagnetic resonance (EPR) spectroscopy of **9** and related structures.[13,14] The advantages and disadvantages of the bis(TMM) approach have been documented elsewhere. In the current context, an additional potential advantage was that the bisdiazene precursors (Figure 6) to bis(TMM)s might be expected to tolerate conditions needed to protonate a pyridine nitrogen. Thus, we chose tetraradicals **10**−**12** and their protonated analogues **13**−**15** as tests of whether pyridines and pyridiniums function as ferromagnetic or antiferromagnetic coupling units. Biradicals **16**−**22** were targeted as important control molecules.

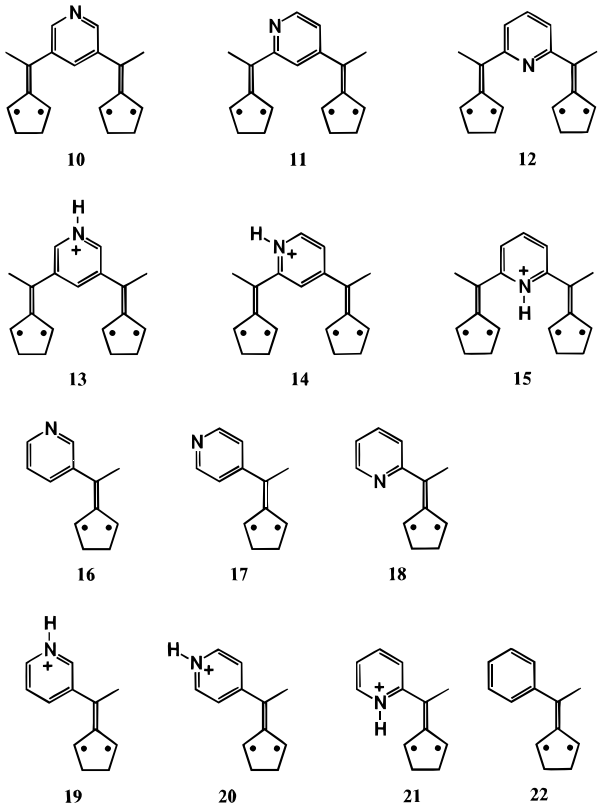

Table 1. Zero-Field Splitting Parameters (cm^{-1}) for Triplet TMMs[a]

	$\|D\|/hc$	$\|E\|/hc$		$\|D\|/hc$	$\|E\|/hc$
16	0.0199	0.002 65	**19** (TFA)	0.0190	0.002 76
17	0.0195	0.002 33	**20** (TFA)	0.0185	0.002 90
18	0.0192	0.002 90	**21** (TFA)	0.0200	0.004 00
			22 (TFA)	0.0195	0.001 75

[a] Determined from the EPR spectra of Figures 7 and 10 after photolysis of the corresponding diazene at 77 K in ethanol.

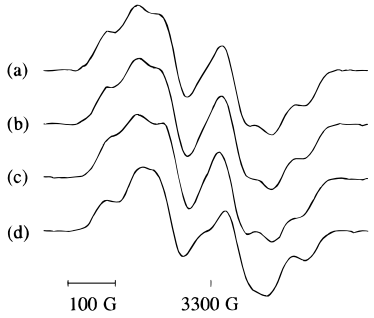

Figure 7. $\Delta m_s = 1$ region of the EPR spectra observed after photolysis of pyridine diazenes at 77 K in ethanol: (a) **18(N2)**; (b) **16(N2)**; (c) **17(N2)**; (d) **22(N2)**.

Synthesis. Syntheses of the neutral, nonprotonated diazene precursors to **10**−**12** (bisdiazenes **10(N2)2**−**12(N2)2**) and **16**−**18** (diazenes **16(N2)**−**18(N2)**) are conceptually straightforward and proceeded smoothly along well-trodden paths.[13,14] The key question was the response of diazenes to the acidic conditions necessary to produce the protonated pyridines.

We have found several sets of conditions which protonate the pyridine nitrogens of the diazene precursors to **10**−**12** and **16**−**18**, but leave the diazene moieties unaffected. These were addition of excess CF_3CO_2H, addition of excess $TsOH{\cdot}H_2O$, addition of excess aqueous HBF_4, and exposure to excess HCl(g), all in ethanol solvent. The most compelling evidence comes from NMR, which showed large downfield shifts of pyridine protons on exposure to acid, and little change elsewhere in the molecule.[15]

EPR Results

Neutral Biradicals. Photolysis of the simple diazenes **16(N2)**, **17(N2)**, and **18(N2)** in either ethanol or 2-methyltetrahydrofuran (MTHF) gave the expected triplet EPR spectra for **16**−**18** (Table 1). The EPR spectra for all three were very similar to each other and to that of the analogous phenyl-TMM **22** (Figure 7). The $\Delta m_s = 1$ spectra are well simulated by published methods.[13] Additionally, all three TMMs exhibit relatively complex $\Delta m_s = 2$ spectra similar to that of **22**.

Neutral Tetraradicals. Photolysis of the neutral bisdiazenes **10(N2)2**, **11(N2)2**, and **12(N2)2** in either ethanol or MTHF followed the now familiar sequence (Figure 6) of first producing a monodiazene triplet biradical which, on extended photolysis, is replaced by a quintet tetraradical (Table 2). The triplet biradicals, produced after short photolysis times by loss of 1 equiv of N_2, show spectra essentially identical to those from the corresponding model biradicals **16**−**18** (Figure 8). Continued photolysis leads in each case to progressive changes in the spectrum, until finally a new spectrum is produced which can be confidently assigned to a quintet tetraradical (Figure 9). Interestingly, the 3,5-isomer **10** gave EPR zero-field splitting (zfs) values almost identical to those for the analogous

(15) Protonation of the diazene would have led to easily measurable shifts in the bridgehead protons, as is commonly seen in azoxy compounds of this class.

Table 2. Zero-Field Splitting Parameters (cm^{-1}) for Quintet Bis(TMM)s[a]

	$\|D\|/hc$	$\|E\|/hc$
(a) **9** (in MTHF)[13]	0.0078	0.0003
(b) **10**	0.0080	0.0003
(in MTHF)	0.0077	0.0003
(c) **11**	0.0084	0.0003
(d) **12**	0.0084	0.0028
(in MTHF)	0.0084	0.0028
(e) **13** (TFA)	0.0083	0.0003
(TsOH)	0.0082	0.0003
(HCl)	0.0083	0.0003
(f) **14** (TFA)[b]	0.0096	0.0003
(HBF_4)	0.0095	0.0003

[a] The zfs parameters were determined from the EPR spectra of Figures 9 and 12 observed after photolysis of the bisdiazenes at 77 K in ethanol, except where indicated. The quintet spectra were simulated using published methods.[13] [b] At either 77 K in the liquid nitrogen dewar or 50 K in the liquid helium cryostat, the zfs parameters for **14** were the same; the two simulations in Figure 12 used only different line widths.

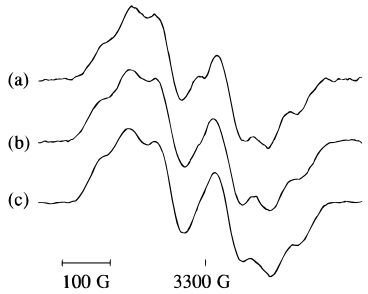

Figure 8. $\Delta m_s = 1$ region of the EPR spectra observed after brief (<5 min) photolysis of pyridinebisdiazenes at 77 K in ethanol: (a) **12**$(N_2)_2$; (b) **10**$(N_2)_2$; (c) **11**$(N_2)_2$.

hydrocarbon tetraradical **9**. However, the 2,4- and 2,6-isomers **11** and **12** both showed measurably different zfs values. In **11** and **12** the perturbing N is in an active (*) position, and it is expected to have a larger influence than in **10**, much as in the **S**−**T** gap calculations (Figure 1). All neutral tetraradicals **10**−**12** gave linear Curie plots over the range 4−70 K, suggesting that all have quintet ground states.

Cationic Biradicals. Although any of the protonation methods mentioned above gave useful EPR spectra, the use of either excess CF_3CO_2H or TsOH in ethanol generally gave the cleanest spectra (fewer doublet impurities), and we will focus on the results from these approaches in our discussion. However, we emphasize that all methods gave qualitatively similar results, and so our conclusions are independent of the counterion to the pyridinium.

The protonated monodiazenes **19**(N_2), **20**(N_2), and **21**(N_2) gave on photolysis conventional triplet EPR spectra corresponding to **19**, **20**, and **21** (Figure 10). Changes in zfs values relative to those of the neutral systems **16**−**18** were generally small but significant (Table 1). As before, pertubations were more noticeable with the 2- and 4-isomers **21** and **20** than with the 3-isomer **19**. These small but observable changes in EPR zfs values provide strong evidence that, in the presence of acid, the biradical produced is different from the neutral analogue. The larger effect with the 2-isomer indicates that the spectral changes are not generic medium effects but instead relate to the specific molecular structures. A linear Curie plot from 4.7 to 50 K was observed for **21**, suggesting a triplet ground state is maintained for the protonated biradical.

To provide further evidence for our protonation method, we prepared NMR samples of **16**(N_2) and **18**(N_2) in ethanol-d_6. After recording ^{1}H NMR spectra, an excess of either CF_3CO_2D or TsOH was added. New ^{1}H NMR spectra revealed exclusive protonation on the pyridine N and thus formation of **19**(N_2) and **21**(N_2). Without dilution, or any further modification, these NMR samples were then degassed, frozen, and photolyzed. The observed EPR spectra were the same as those from conventional EPR samples.

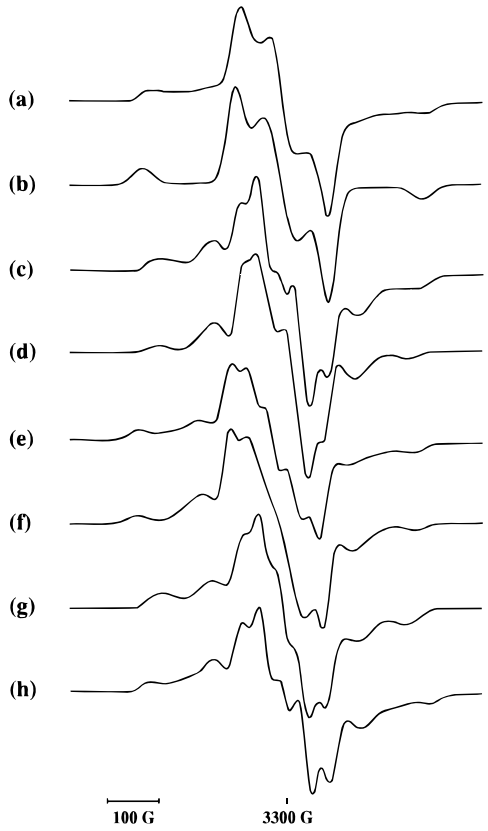

Figure 9. $\Delta m_s = 1$ region of the EPR spectra observed after extended (>3 h) photolysis of bisdiazenes at 77 K in ethanol: (a) **12**$(N_2)_2$; (b) simulation of **12**; (c) **10**$(N_2)_2$; (d) simulation of **10**; (e) **11**$(N_2)_2$; (f) simulation of **11**; (g) **9** from ref 13; (h) **13**$(N_2)_2$, TFA counterion. Simulation zfs values are from Table 2.

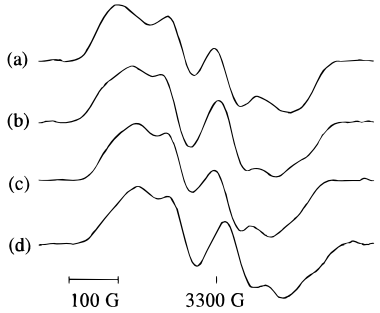

Figure 10. $\Delta m_s = 1$ region of the EPR spectra observed after photolysis of pyridiniumdiazenes (TFA) at 77 K in ethanol: (a) **21**(N_2); (b) **19**(N_2); (c) **20**(N_2); (d) **13**$(N_2)_2$ (brief photolysis).

The evidence from the model compounds **16**−**20** indicates that we have achieved our design goal. We can protonate pyridine-containing diazenes on the pyridine N. On photolysis, these structures lose N_2 from the diazene to produce a biradical with the pyridine N still protonated. In these systems, protonating the pyridine N introduces only a minor perturbation. With this background, we can proceed to the analysis of the protonated tetraradicals.

Cationic Tetraradicals. Photolysis of protonated, 3,5-substituted bisdiazene **13**$(N_2)_2$ led to a sequence almost identical to that for the neutral hydrocarbon (or pyridine) analogue **9**$(N_2)_2$

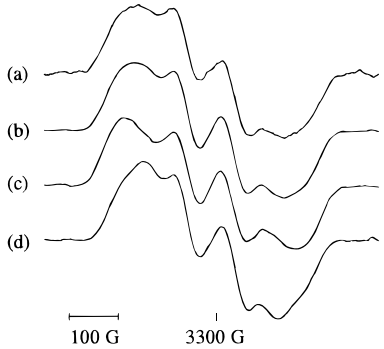

Figure 11. $\Delta m_s = 1$ region of the EPR spectra observed after photolysis at 77 K in ethanol: (a) **14(N$_2$)$_2$**, TFA counterion, 20 s photolysis; (b) predicted spectrum obtained by adding the experimental spectra of **21** (c) and **20** (d) in a 1:1 mole ratio. Spectra in (c) and (d) are the same as in Figure 10a,c.

(or **10(N$_2$)$_2$**). Short photolysis times produced a triplet EPR spectrum almost identical to that for the model protonated biradical **19** (Figure 10). Continued photolysis led to a quintet spectrum (Figure 9), again very similar to that of the hydrocarbon **9** or neutral pyridine **10**. Linear Curie behavior was seen from 4.3 to 70 K, consistent with a quintet ground state for **13**.

After brief photolysis, protonated 2,4-substituted bisdiazene **14(N$_2$)$_2$** can give rise to two different TMM biradicals. Indeed, brief photolysis produces an EPR spectrum that is different from that of either model compound **20** or **21**, but is well matched by the spectrum obtained by summing the experimental spectra of **20** and **21** in a 1:1 mole ratio (Figure 11). Such behavior from an unsymmetrical bisdiazene precursor to a bis(TMM) has been seen previously.[14]

Extended photolysis of **14(N$_2$)$_2$** leads to a new spectrum which, while measurably different from those of the neutral analogues **9**−**12**, is still clearly a member of the same class of bis(TMM) quintet tetraradicals (Figure 12). The spectral line widths, but not the zfs parameters (Table 2), show a medium effect (Figure 12). A Curie plot (using either double-integral areas or peak−peak heights) was linear from 4.4 to 70 K.

Thus far, the five bis(TMM) systems discussed above (**10**−**14**) and several others we have described previously[13,14] follow a consistent pattern, involving generation of a triplet TMM biradical spectrum that gradually evolves into a quintet spectrum. However, upon photolysis, protonated 2,6-substituted bisdiazene **15(N$_2$)$_2$** consistently and reproducibly gives rise to a series of spectra that are quite different from those seen from all previous systems. The initial behavior is standard. Brief photolysis produces a triplet TMM with spectral parameters very similar to those of the model compound **21**. It is on extended photolysis that new behaviors are seen.

In other systems of this type, continued photolysis leads to two changes. First, new lines corresponding to the quintet tetraradical appear. Second, the *overall* EPR signal intensity steadily rises: all lines increase in intensity, but the quintet grows more rapidly and ultimately dominates the spectrum. As shown in Figures 13−15, the behavior of the **15** system is anomalous with regard to both behaviors.

The results are best summarized by the stacked plot of Figure 13. The initial triplet spectrum (assigned to **15(N$_2$)**) is *replaced* by a new spectrum. The overall EPR intensity does not show the steady increase of other systems (Figure 14). After an initial steep rise—at which point the spectrum is that of biradical **15(N$_2$)**—the total intensity levels off.[16] Upon continued photolysis there are progressive changes in the spectral shape, but no significant intensity increase.

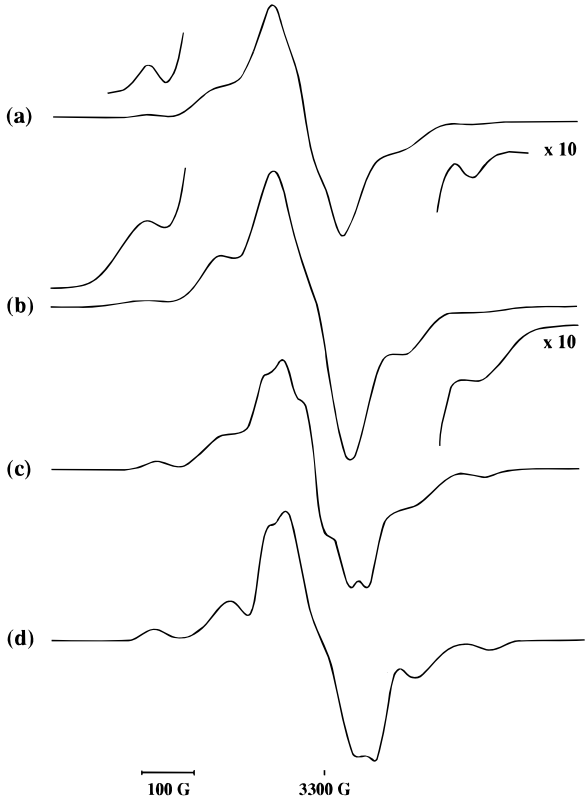

Figure 12. $\Delta m_s = 1$ region of the EPR spectra observed after extended (>3 h) photolysis of bisdiazene **14(N$_2$)$_2$** in ethanol, TFA counterion: (a) photolysis at 77 K in liquid nitrogen; (b) simulation of (a); (c) photolysis at 50 K in the liquid helium cryostat; (d) simulation of (c). Simulation zfs values are from Table 2.

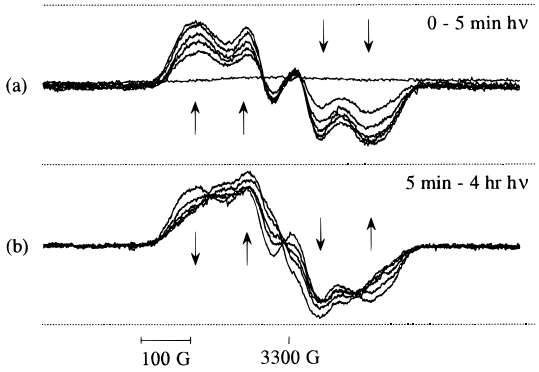

Figure 13. Stack plots of the $\Delta m_s = 1$ region of the EPR spectra observed upon photolysis of **15(N$_2$)$_2$**,TFA counterion, in ethanol at 77 K: (a) 0−5 min photolysis; (b) 5 min to 4 h photolysis. The spectrometer gain was unchanged during the experiment. The arrows show the direction of change in the indicated peak intensities with time.

The final spectrum (Figure 15b) noticeably lacks the outer wings that are prominent in the spectra all six previously observed bis(TMM) quintet tetraradicals of this family (**9**−**14**). One can, however, simulate the final spectrum as that of a triplet species (Figure 15c). The simulated zfs D value ($|D|/hc = 0.015$ cm^{-1}) is somewhat smaller than those of the TMM biradicals **16**−**22**, but still in the range of that of a substituted TMM.

There are some complications in the study of **15(N$_2$)$_2$**. The spectra of Figures 13 and 15a,b were obtained by photolysis at 77 K in a liquid N_2 dewar, a standard condition for such systems.

(16) The kinetics in Figure 14 suggest that the protonated diazenes lose N_2 upon photolysis more rapidly than their neutral analogues. This is supported by an experiment in which matched photolyses of **21(N$_2$)** and **18(N$_2$)** revealed a 2−3-fold faster photolysis rate for **21(N$_2$)**.

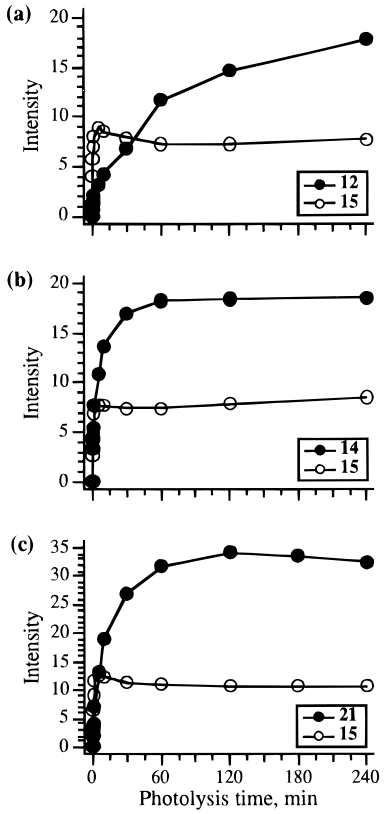

Figure 14. Kinetic plots for the compared photolyses of **15(N$_2$)$_2$** (open symbols) and several other compounds (closed symbols). The intensities are of the double-integrated $\Delta m_s = 1$ spectra (in arbitrary units); the $\Delta m_s = 2$ spectra gave qualitatively similar plots. Lines connecting the points are for illustration only. See the Experimental Section for details.

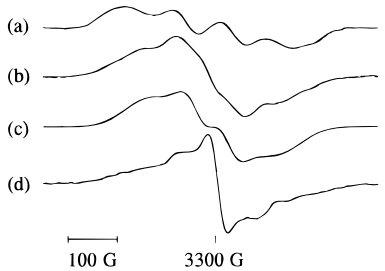

Figure 15. $\Delta m_s = 1$ region of the EPR spectra observed after photolysis of 15**(N$_2$)$_2$** in ethanol: (a) 1 min photolysis at 77 K in liquid nitrogen, tosylate counterion; (b) 4 h photolysis at 77 K in liquid nitrogen, tosylate counterion; (c) Simulation of a triplet with zfs parameters $|D|/hc = 0.015$, $|E|/hc = 0.0030$ cm^{-1}; (d) 6 h photolysis at 50 K in the liquid helium cryostat, TFA counterion.

However, photolysis at 50 K in a liquid He cryostat (Figure 15d) gives a slightly different and relatively uninformative spectrum. The new central feature could result from the development of doublet (monoradical) impurities introduced by secondary photolysis of bi- or tetraradicals. Such behavior has not been seen in any other structures of this type. A Curie plot for the $\Delta m_s = 1$ spectrum from Figure 15d is linear from 3.9 to 70 K, although, given the strong central feature, the significance of this result is unclear. We emphasize that the differing behaviors seen in the two different photolysis setups are completely reproducible.

Discussion

The *m*-phenylene ferromagnetic coupling unit has been the workhorse in studies of high-spin organic molecules, and our theoretical studies make some interesting predictions concerning this system. First, replacing the benzene by a neutral pyridine should have a minimal effect on spin coupling. However, a pyridinium can have a substantial effect, depending on the substitution pattern.

As expected, the perturbation in **4** is minimal because the NH^+ is introduced at an inactive (non-*) site. However, when the NH^+ is placed at an active (*) site, substantial perturbations arise. In **5**, the **S** and **T** states are very close. In **6** there would appear to be a preference for **S**, although the energy differences are relatively small. Certainly, the dication **7** is expected to be low spin.

The theoretical results can be rationalized with either VB or MO arguments. In **5** and **6**, the NH^+ preferentially stabilizes the singlet state by introducing closed-shell, "ionic" resonance structures. Alternatively, the NH^+ opens up a HOMO−LUMO gap, again preferentially stabilizing **S**.

We have made a considerable effort to experimentally test the theory. We have studied a number of model systems and performed extensive control experiments that convince us that the bis(TMM) approach is useful in this context. We have established that we can preferentially protonate a pyridine N in the presence of a bicyclic diazene, and we can generate biradicals and tetraradicals containing pyridiniums.

Overall, our observations provide good, general support for the theory. Both spectroscopically and energetically, a neutral pyridine appears to be a minor perturbation relative to a benzene, regardless of the substitution pattern. Spectroscopically, there is a consistent trend in both neutral and ionic systems that a substitution pattern analogous to **4** is only minimally perturbing, while substitution patterns corresponding to **5** and **6** present measurable perturbations. Also, the cationic tetraradical **13** appears in all ways to be quite similar to the neutral pyridine (**10**) and hydrocarbon (**9**) analogues, consistent with the theoretical prediction for **4**.

Of course, the most interesting systems are cationic tetraradicals **14** and **15**. The 2,4-isomer **14** is well behaved and has a quintet ground state. This indicates that biradical **5** has a triplet ground state. This is not inconsistent with theory, which made no firm prediction concerning the ground state of **5**. Also, it must be remembered that the calculations consider planar molecules in the gas phase, while the bis(TMM)s are nonplanar[17] and are studied in a condensed, polar medium.[18]

Still, given the predicted small **S**−**T** gap for **5**, one might have expected to see thermal population of the triplet state of **14**. We see no evidence for this. In favorable cases, the bis(TMM) strategy has been used to detect higher lying states, even if fairly substantial energy gaps are involved. However, in the current systems the spectra are relatively broad, and the spectra of thermally populated triplet states are expected to overlap extensively with the quintet spectra. We estimate that

(17) On the basis of X-ray structures of model compounds and theoretical calculations, we estimate that in systems such as **9**−**15** the twist around the $C_{aryl}-C_{TMM}$ bond could be as large as 37°.[14] How should twisting affect spin preferences? The singlet-stabilizing resonance structures of Figure 3 introduce double bond character to the bond of interest, and so one might expect that twisting would preferentially destabilize the singlet. Indeed, preliminary calculations on **6** indicate that the singlet is more sensitive to twisting, and a similar trend should hold for **5**. We have attempted to prepare an analogue of **15** that is constrained to be planar, by tying back the methyl groups to the pyridine in five-membered rings. However, we were unable to synthesize the bisdiazene.

(18) The influence of these perturbations is more difficult to evaluate. One might expect, though, that a polar medium and/or hydrogen bonding with the pyridinium hydrogen would tend to decrease the effective charge at the nitrogen. This would diminish the NBMO splitting and thereby lessen the preferential stabilization of the singlet that protonation produces. Preliminary calcualtions involving the hydrogen-bonded complex **6**·H_2O indicate that the preference for a singlet ground state may be reduced by as much as several kilocalories per mole.

we would need an equilibrium population of at least 30% of a triplet species to be able to see it clearly in this system.[19] Using previously developed arguments,[13] our inability to do so requires an **S**−**T** gap of only 0.5 kcal/mol for **5**.

The results for **15** are more complicated. However, one thing is clear: the system for which theory most strongly predicted a deviation from standard behavior is, in fact, different from all other bis(TMM)s studied to date. Further interpretation might be considered incautious: the spectra are broad, weak, and sometimes complicated by features that may be due to monoradical impurities.

Nevertheless, on the basis of the data of Figures 13−15, we feel we can present a consistent and plausible interpretation of our observations for **15**. We propose that cation tetraradical **15** has a *triplet* ground state.[20] This surprising result is contrary to our previous analysis of the bis(TMM) strategy.[13] Earlier, we invoked a Heisenberg Hamiltonian for the interaction of two triplet biradicals through a potential coupling unit. In this model, two energy orderings are possible, **Q** < **T** < **S** or **S** < **T** < **Q**, depending on whether the intervening structure is a ferromagnetic coupling unit or an antiferromagnetic coupling unit, respectively. A **T** ground state is impossible in this scheme. However, this approach is appropriate only if the coupled biradicals retain their triplet character.[13] In **15**, the resonance structures analogous to those involved for **6** (Figure 3) include structures such as **15a**. Clearly, the TMM units have

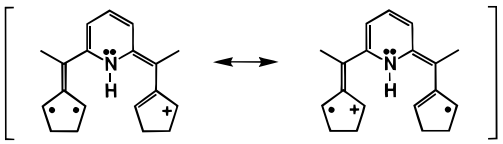

15a

been disrupted, and so the simple (**T** + **T**) Heisenberg Hamiltonian used here may be inappropriate. Presumably, a more complete Hamiltonian considering all four electrons individually would be applicable, but we do not have enough quantitative data to evaluate such a model.

The resonance structures explicitly depicted in **15a** are but two of a large number of *biradical* forms available to **15**. The overall topology does appear to be high spin—note the TMM substructure in the left form—although the applicability of the π-topology rules to charged π-systems is uncertain. While it is difficult to predict the EPR spectroscopy of such a triplet, it is reasonable to assume that the *D* value would be less than those for TMMs such as **16**−**22**, due to the greater delocalization. This is what is observed spectroscopically.

Of course, resonance structures analogous to **15a** are also available to **14**. Yet spectroscopically, **14** appears to be a conventional bis(TMM) tetraradical, rather than a biradical such as **15a**. This is consistent with the greater resonance stabilization in ^{1}**6** than ^{1}**5**, and thus a greater benefit to forming biradical structures **15a**.

Our experiments thus suggest that a 2,6-disubstituted pyridinium is *not* a ferromagnetic coupling unit. Instead, two simple radicals linked through such a unit should antiferromagnetically couple, producing a singlet ground state. Concerning the bis(TMM) strategy, we have previously seen a *hydrocarbon* system antiferromagnetically couple two TMMs to produce a singlet ground state,[13] consistent with the Heisenberg Hamiltonian. In the current system, because of strong ionic contributions, "antiferromagnetic coupling" of two triplets appears to produce a triplet.

Conclusion

Theory clearly predicts that, while pyridines are only subtly different from a benzene in magnetic coupling, pyridiniums can be quite different. When the pyridinium NH^+ is substituted into an active site of *m*-xylylene, ionic contributions to the singlet wave function are greatly increased, causing a substantial reduction in the **S**−**T** gap. These theoretical predictions have been experimentally tested using the bis(TMM) strategy. Overall, the agreement between theory and experiment is very good. This includes support for the theoretical prediction of violation of the high-spin topology rules for a 2,6-pyridinium system.

Experimental Section

Computational Methodology. Full geometry optimizations in C_{2v} were carried out for the two lowest-lying states ($^3B_2$ and $^1A_1$) of **1**, **3**, **4**, **6**, **7,** and **8** using either the 6-31G* or 6-31G basis set.[21] Geometry optimizations were likewise performed on **5** using C_s symmetry. Geometries of triplet states were optimized at the UHF level; singlet states were done at the GVB(1/2), or two-configuration SCF, level. These geometry optimizations were performed with the Gaussian 92 package of *ab initio* programs.[22]

Starting from the ROHF wave functions for the triplet states and the GVB(1/2) wave functions for the singlet species, single-point CI calculations including all single and double excitations in the π-space from one reference configuration of triplet states, and from two configurations for singlets, were performed at each state's optimized geometry.[23] The basis set used for CI calculations was always the same as that used for the respective geometry optimization. Table 3 shows the calculated energies and gaps at the highest level of theory examined for each molecule. Calculations were also done at the 6-31G/8π full CI and 6-31G*/32π CCCI[24] levels with qualitatively similar results.

General Procedures. Reactions were performed under an argon atmosphere. Tetrahydrofuran was distilled from sodium−benzophenone ketyl. Methylene chloride was distilled from CaH_2. Reported yields refer to material dried to constant weight under vacuum, typically 50 mTorr. Flash chromatography was performed on 230−400 mesh silica gel with the solvent indicated. All NMR shifts are reported as δ (ppm)

(19) Recall that the $\Delta m_s = 1$ EPR signal intensity scales as $S(S+1)$, and so quintet spectra are inherently more intense than triplet spectra by a factor of 3.

(20) An alternative explanation is that the **S**, **T**, and **Q** states of **15** are nearly degenerate, and the spectra of Figure 15 reflect a mixture of **Q** and **T** spectra. While plausible, we consider this explanation unlikely for the following reasons. First, on the basis of the precedent of six other bis(TMM)s of this type (**9**−**14**), we can anticipate the spectroscopy of such a situation, and the narrowness of the spectra of Figure 15 is inconsistent with expected *D* values. Also, the spectral shape is not consistent with those of all the other systems. Finally, because quintet spectra are inherently more intense than triplet spectra,[19] this model is inconsistent with the kinetics of Figure 14. That is, following the initial rise corresponding to formation of biradical **15(N$_2$)**, evolution to a mixture of tetraradical **Q** and **T** states *must* lead to an overall increase in spectral intensity, by a factor of 2 if a statistical mixture of **Q**, **T**, and **S** is formed, and by as much as a factor of 3 if only **Q** is formed.

(21) For molecule **8** there appear to be two low-lying singlet states: one $^1A_1$ state and one $^1B_2$ state. At the π-CISD level, the $^1B_2$ state, at its optimized geometry, is less than 1 kcal/mol higher in energy than the $^1A_1$ state (at its own optimized geometry). Thus, from our level of theory we are unable to determine which state is the lowest singlet. The ordering of these singlet states seems to be intermediate in character between that observed for **1** ($^1A_1$ state below $^1B_2$ by ∼10 kcal/mol) and that observed for *m*-quinone[4] ($^1B_2$ state below $^1A_1$ by ∼10 kcal/mol).

(22) Gaussian 92, Revision C: M. J. Frisch, G. W. Trucks, M. Head-Gordon, P. M. W. Gill, M. W. Wong, J. B. Foresman, B. G. Johnson, H. B. Schlegel, M. A. Robb, E. S. Replogle, R. Gomperts, J. L. Andres, K. Raghavachari, J. S. Binkley, C. Gonzalez, R. L. Martin, D. J. Fox, D. J. Defrees, J. Baker, J. J. P. Stewart, and J. A. Pople, Gaussian, Inc., Pittsburgh, PA, 1992.

(23) The CI calculations were carried out using the MQM:CI2P5 program: Bobrowicz, F. W.; Goodgame, M. M.; Bair, R. A.; Walch, S. P.; Goddard, W. A., III; unpublished work. Bobrowicz, F. W. Ph.D. Thesis, California Institute of Technology, 1974.

(24) Carter, E. A.; Goddard, W. A., III. *J. Chem. Phys.* **1988**, *88*, 1752−1763, 3132−3140.

Table 3. Energies and Singlet−Triplet Gaps of **1** and **3**−**8**

molecule	ROHF E_T, hartrees[a]	GVB(1/2) E_S, hartrees	π-CISD E_T, hartrees[b]	π-CISD $E_S - E_T$, kcal/mol
1	−307.5220	−307.5227	−307.6289	9.42
3[c]	−323.3934	−323.3954	−323.4953	8.80
4	−323.8932	−323.8944	−323.9992	6.24
5	−323.9054	−323.9137	−324.0061	−0.028
6	−323.9053	−323.9131	−324.0063	−2.37
7	−340.0838	−340.1213	−340.1772	−23.14
8[c]	−339.9835	−339.9808	−340.0842	11.33

[a] UHF energies at the UHF optimized geometry of **1**, and **3**−**8** were −307.5755, −323.4475, −323.9362, −323.9408, −323.9404, −340.1015, and −340.0276, respectively. [b] Single and double CI in the π-space, with one reference configuration for triplet states and two for singlets. [c] 6-31G//6-31G; otherwise 6-31G*//6-31G*.

Scheme 1

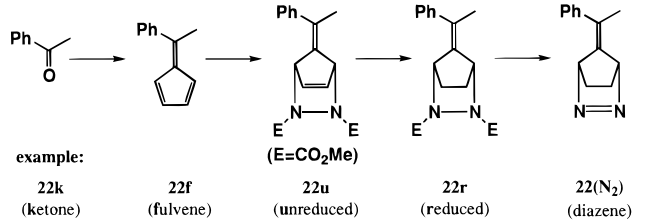

downfield from TMS. ^{1}H NMR spectra were recorded at 300 MHz in $CDCl_3$ and ^{13}C NMR spectra at 75 MHz in $CDCl_3$ using a GE QE-300 spectrometer, except where noted. ^{1}H NMR spectra at 400 MHz were obtained with a JEOL GX-400 spectrometer. A range of peak positions indicates a multiplet of poorly resolved lines. IR spectra were recorded on a Perkin-Elmer 1600 series instrument. MS refers to a 70 eV EI mass-selective detector (HP 5970) coupled to a HP 5890 GC unless otherwise indicated. Relative mass abundances (%) are given in parentheses (100 = base peak). FAB-MS, DEI-MS, 50 eV EI-MS, and HRMS determinations were performed at the University of California, Riverside. UV spectra were taken using a Beckman DU-640 spectrometer. Elemental analysis was performed at Atlantic Microlabs, Norcross, GA. Melting points were obtained on a Thomas-Hoover apparatus and are uncorrected. EPR samples were prepared in 2-methyltetrahydrofuran (MTHF; refluxed over CaH_2, distilled, and vacuum transferred from sodium−benzophenone ketyl) or ethanol (absolute, used as received) and degassed with several freeze−pump−thaw cycles. EPR spectra were acquired on a Varian E-line Century Series EPR spectrometer at 100 kHz modulation frequency, X-band microwave frequency 9.18−9.29 GHz. $\Delta m_s = 1$ spectra were observed centered at $g = 2.00$; simulations used $g = 2.0023$. A liquid nitrogen finger dewar was used for experiments at 77 K. An Oxford Instruments ESR-900 liquid helium cryostat was used for variable-temperature experiments (4 K and higher). Samples were photolyzed in the EPR cavity with the filtered, focused output (usually ∼307−386 nm) of a 500 W Hg arc lamp. Lamps, housings, lenses, and power supplies were obtained from Oriel Corp., Stratford, CT. Filters were obtained from Schott Optical Glass Co., Duryea, PA. The pyridyl monoketones are commercially available, as is 2,6-diacetylpyridine.

General Route to Diazenes. The diazene precursors to all the TMMs were synthesized via similar routes, as illustrated for **22(N$_2$)** in Scheme 1. The ketone starting material was converted to the fulvene, which was reacted with dimethyl azodicarboxylate (DMAD) and reduced to the biscarbamate. This was hydrolyzed and oxidized to the diazene. All diazenes were stored at −20 °C in CH_2Cl_2 solution.

General Preparation of fulvenes. Two methods of synthesizing fulvenes from ketones were employed. (1) The ketone was stirred with cyclopentadiene and pyrrolidine in methanol at room temperature.[25] (2) The ketone was stirred with CpMgBr in refluxing THF. CpMgBr was prepared from MeMgBr and cyclopentadiene and was assumed to have an effective MW of 400.[26] For the pyridyl ketones the first method often worked somewhat better, although the yields in both cases were

Scheme 2

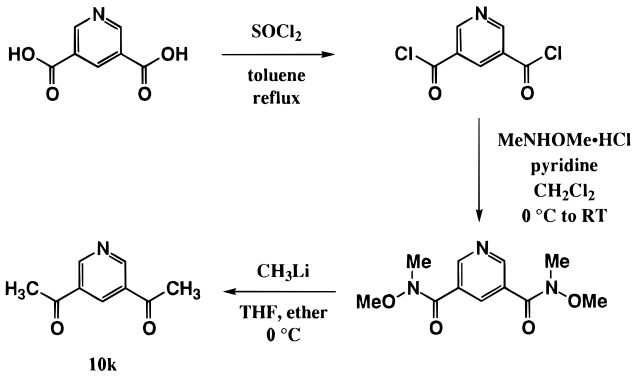

routinely low. Representative procedures using both methods are given below.

General Preparation of Reduced DMAD Adducts. The fulvene was reacted with a slight excess of DMAD in CH_2Cl_2 at room temperature and then reduced with diimide generated from potassium azodicarboxylate (PADC). In one instance (**10u**) the intermediate unreduced DMAD adduct was isolated.

General Preparation of Diazenes. The reduced DMAD adduct was refluxed with KOH in isopropyl alcohol and then oxidized with nickel peroxide[27] (NiO_x) in CH_2Cl_2 at 0 °C.

Preparation of Ketone Starting Materials. The 3,5- and 2,4-diacetylpyridines (**10k** and **11k**) were synthesized from the corresponding dicarboxylic acids by conversion to the acid chlorides, amidation to the bis(Weinreb amide)[28] with *N*,*O*-dimethylhydroxylamine, and alkylation with methyllithium (see Scheme 2). Procedures are given below.

3,5-Pyridinedicarbonyl Chloride. 3,5-Pyridinedicarboxylic acid (7.0 g, 0.042 mol) and 15 mL of $SOCl_2$ (0.21 mol) were refluxed in 300 mL of toluene under a Drierite drying tube for 19 h. The solution was cooled to room temperature, and the solvent was rotoevaporated, providing an off-white solid which solidified on standing. The dried crude material was used directly in the next step.

3,5-Pyridinediamide. The crude dichloride was dissolved in 250 mL of CH_2Cl_2 under argon. MeNHOMe·HCl (9.24 g, 0.0947 mol, 1.1 equiv/equiv of chloride) was added, and the mixture was stirred for ∼30 min, after which time nearly all the solid dissolved, giving a yellow-orange solution. Pyridine (15.0 mL, 0.185 mol, 2.2 equiv/equiv of chloride) was added dropwise to the ice-cooled solution, which was allowed to warm to room temperature. After 30 min the mixture was poured into 200 mL of water, and the aqueous layer was made basic (pH ≥ 10) with 10% aqueous KOH. The orange layers were shaken and separated, and the aqueous layer was extracted with 2 × 100 mL of CH_2Cl_2. The organic layers were combined, washed with 100 mL of saturated aqueous NaCl, dried ($MgSO_4$), and filtered. The pale yellow filtrate was rotoevaporated, and traces of pyridine were removed on the vacuum pump, affording 9.15 g of a tan solid (86% from 3,5-pyridinedicarboxylic acid): ^{1}H NMR δ 9.0 (s, 2H), 8.35 (s, 1H), 3.6 (s, 6H), 3.4 (s, 6H); MS *m/z* ($M^{\bullet+}$) 253 (5), 194 (11), 193 (100), 134 (28), 105 (57), 77 (49), 50 (37).

3,5-Diacetylpyridine (10k). The diamide (9.15 g, 36.1 mmol) was dissolved in 250 mL of THF under argon and cooled in an ice−water bath. Methyllithium (100 mL of 1.4 M MeLi in ether, 0.14 mol, 1.9 equiv/equiv of amide) was cannulated into the solution in a steady stream. The solution immediately turned cloudy and light orange. After 1 h the mixture was poured onto 100 mL of water containing 9 mL of concentrated HCl. The layers were shaken vigorously and separated (pH of aqueous layer ≥ 10). The aqueous layer was extracted with 3 × 100 mL of ether and then rotoevaporated to remove THF. The aqueous layer was extracted with an additional 100 mL of ether, and all the organic layers were combined, dried ($MgSO_4$), and filtered. The orange filtrate was rotoevaporated to an oil and dried to give 5.9 g of an orange solid. This was chromatographed (1:2 hexanes−ethyl

(25) Stone, K. J.; Little, R. D. *J. Org. Chem.* **1984**, *49*, 1849−1853.
(26) Stille, J. R.; Grubbs, R. H. *J. Org. Chem.* **1989**, *54*, 434−444.
(27) Snyder, G. J.; Dougherty, D. A. *J. Am. Chem. Soc.* **1985**, *107*, 1774−1775.
(28) Nahm, S.; Weinreb, S. M. *Tetrahedron Lett.* **1981**, *39*, 3815−3818.

acetate), providing a yellow solid which was recrystallized from 3:1 hexanes−ethyl acetate to afford white needles, 3.46 g (59%), mp 68.5−70.5 °C (lit.[29] mp 72 °C). The mother liquor from the recrystallization was concentrated and recrystallized, providing a second crop of very pale yellow needles, 0.38 g (total yield 65%): ^{1}H NMR δ 9.33 (s, 2H), 8.72 (s, 1H), 2.70 (s, 6H); ^{13}C NMR δ 195.83, 152.94, 134.71, 131.95, 26.75; IR (NaCl plate, film) 1692 cm^{-1}; MS *m/z* ($M^{\bullet+}$) 163 (28), 148 (62), 120 (42), 43 (100); HRMS for $C_9H_9NO_2$, calcd 163.0633, found 163.0637. Anal. Calcd for $C_9H_9NO_2$: C, 66.25; H, 5.56; N, 8.58. Found: C, 66.31; H, 5.61; N, 8.60.

2,4-Pyridinedicarbonyl Chloride. 2,4-Pyridinedicarboxylic acid monohydrate (5.0 g, 0.027 mol) and 10 mL of $SOCl_2$ (0.137 mol) were refluxed in 200 mL of toluene under a Drierite drying tube for 16 h. The dark brown solution was cooled to room temperature and rotoevaporated to a clear black oil. The material, 5.6 g, solidified on drying and was used directly in the next step.

2,4-Pyridinediamide. The crude dichloride was dissolved in 150 mL of CH_2Cl_2 under argon. MeNHOMe·HCl (5.79 g, 0.0593 mol, 1.1 equiv/equiv of chloride) was added, and the mixture was stirred for ∼30 min, after which time nearly all the solid dissolved, giving a brown-black solution. Pyridine (9.6 mL, 0.119 mol, 2.2 equiv/equiv of chloride) was added dropwise to the ice-cooled solution, which was allowed to warm to room temperature. After 45 min the black mixture was rotoevaporated to a black solid. Water and CH_2Cl_2 (100 mL each) were added, and the aqueous layer was made basic (pH ≥ 10) with 10% aqueous KOH. The layers were shaken and separated. The dark red-brown aqueous layer was extracted with 2 × 75 mL of CH_2Cl_2. The organic layers were combined, washed with 75 mL of saturated aqueous NaCl, dried ($MgSO_4$), and filtered. The red-brown filtrate was rotoevaporated, and the residue was chromatographed (1:2 hexanes−ethyl acetate to 1:9 methanol−ethyl acetate), affording 6.57 g of a light brown oil (96% from 2,4-pyridinedicarboxylic acid monohydrate): ^{1}H NMR δ 8.71 (d, J = 5.0 Hz, 1H), 7.89 (br s, 1H), 7.61 (dd, J = 5.0, 1.5 Hz, 1H), 3.74 (s, 3H), 3.57 (s, 3H), 3.42 (s, 3H), 3.38 (s, 3H); ^{13}C NMR δ 166.54, 153.02, 148.54, 142.13, 122.91, 121.41 (br), 61.24, 32.79 (br); MS *m/z* ($M^{\bullet+}$) 222 (75), 193 (22), 165 (100), 77 (45); DEI-MS *m/z* ($[M + H]^+$) 254 (32), 222 (100), 194 (31), 165 (94), 77 (59); HRMS for ($[M + H]^+$) $C_{11}H_{16}N_3O_4$, calcd 254.1141, found 254.1141.

2,4-Diacetylpyridine (11k). The diamide (6.48 g, 25.6 mmol) was dissolved in 175 mL of THF under argon and cooled in an ice−water bath. Methyllithium (50 mL of 1.4 M MeLi in ether, 0.070 mol, 1.4 equiv/equiv of amide) was cannulated into the solution in a steady stream. The solution immediately turned cloudy and light orange. After 1 h the mixture was poured onto 100 mL of water containing 5 mL of concentrated HCl. The layers were shaken vigorously and separated (pH of aqueous layer ≥ 10). The aqueous layer was extracted with 2 × 50 mL of ether, and the organic layers were combined, dried ($MgSO_4$), filtered, and rotoevaporated to a light brown solid. This was chromatographed (2:1 hexanes−ethyl acetate), providing 2.96 g (71%) of an off-white solid, mp 71.0−72.0 °C (lit.[30,31] mp 71 °C). ^{1}H NMR δ 8.88 (dd, J = 5.0, 0.8 Hz, 1H), 8.44 (dd, J = 1.7, 0.8 Hz, 1H), 7.94 (dd, J = 5.0, 1.7 Hz, 1H), 2.77 (s, 3H), 2.69 (s, 3H); ^{13}C NMR δ 199.32, 196.65, 154.68, 150.14, 143.70, 124.02, 119.38, 26.71, 25.81; IR (NaCl plate, film) 1698 cm^{-1}, lit.[31] (KBr) 1695 cm^{-1}; MS *m/z* ($M^{\bullet+}$) 163 (100), 121 (84), 120 (60); HRMS for $C_9H_9NO_2$, calcd 163.0633, found 163.0640. An analytical sample was recrystallized from hexanes. Anal. Calcd for $C_9H_9NO_2$: C, 66.25; H, 5.56; N, 8.58. Found: C, 66.08; H, 5.50; N, 8.52.

Representative Preparation of Fulvenes Using Cyclopentadiene and Pyrrolidine in Methanol. 6-(2-Pyridyl)-6-methylfulvene (18f). 2-Acetylpyridine (1.00 mL, 8.92 mmol) was dissolved in 9 mL of methanol under argon. Cyclopentadiene (1.9 mL, 23.1 mmol, 2.6 equiv) and pyrrolidine (4.1 mL, 45.3 mmol, 5.1 equiv) were added, and the solution was stirred. After 16 h the dark brown solution was quenched with 2.8 mL of acetic acid (48.9 mmol, 5.5 equiv) and then 10 mL each of water and saturated aqueous NaCl. The brown mixture was extracted with 4 × 20 mL of ether. The organic extracts were combined, washed with 20 mL of saturated aqueous NaCl, dried ($MgSO_4$), and filtered. The filtrate was rotoevaporated and chromatographed (10:1 hexanes−ethyl acetate), providing 0.631 g (42%) of an orange oil. Preparation using CpMgBr (see below) gave a 23% yield: ^{1}H NMR δ 8.65 (ddd, J = 4.8, 1.8, 1.2 Hz, 1H), 7.66 (td, J = 7.8, 1.8 Hz, 1H), 7.38 (dt, J = 7.8, 1.0 Hz, 1H), 7.21 (ddd, J = 7.8, 1.0 Hz, 1H), 6.66 (ddd, J = 5.3, 2.0, 1.6 Hz, 1H), 6.55 (dt, J = 5.3, 1.6 Hz, 1H), 6.49 (dm, J = 5.3 Hz, 1H), 6.26 (ddd, J = 5.3, 2.0, 1.6 Hz, 1H), 2.60 (s, 3H); ^{13}C NMR δ 159.00, 148.99, 147.42, 144.22, 135.46, 132.16, 125.20, 122.97, 122.49, 121.53, 20.67; MS *m/z* ($M^{\bullet+}$) 169 (90), 168 (100), 167 (89), 154 (62); HRMS for $C_{12}H_{11}N$, calcd 169.0891, found 169.0886; UV (CH_2Cl_2) λ_{max} 297, ∼379 (sh) nm.

Representative Preparation of Fulvenes Using CpMgBr. 6-(3-Pyridyl)-6-methylfulvene (16f). 3-Acetylpyridine (0.50 mL, 4.55 mmol) and 5.46 g of CpMgBr (3 equiv) were refluxed in 50 mL of THF for 6 h. The cooled mixture was quenched with 50 mL of saturated aqueous NH_4Cl and 10 mL of water. The layers were shaken and separated, and the aqueous layer was extracted with 25 mL of ether. The organic layers were combined, dried ($MgSO_4$), and filtered. The filtrate was rotoevaporated and chromatographed (2:1 hexanes−ethyl acetate), affording 0.349 g (45%) of an orange oil. Preparation with cyclopentadiene/pyrrolidine (see above) gave a 28% yield: ^{1}H NMR δ 8.62 (m, 1H), 8.58 (dd, J = 4.8, 1.4 Hz, 1H), 7.66 (dm, J = 8.0 Hz, 1H), 7.29 (m, 1H), 6.61 (m, 1H), 6.58 (m, 1H), 6.49 (dm, J = 5.1 Hz, 1H), 6.10 (ddd, J = 5.1, 2.1, 1.5 Hz, 1H), 2.51 (s, 3H); ^{13}C NMR δ 149.41, 148.86, 144,83, 144.25, 137.17, 135.76, 132.34, 132.22, 122.65, 122.46, 120.68, 21.97; MS *m/z* ($M^{\bullet+}$) 169 (54), 168 (100), 167 (43), 154 (30); HRMS for $C_{12}H_{11}N$, calcd 169.0891, found 169.0887; UV (CH_2Cl_2) λ_{max} 298, ∼377 (sh) nm.

6-(4-Pyridyl)-6-methylfulvene (17f). 4-Acetylpyridine (1.00 mL, 8.92 mmol) was dissolved in 9 mL of methanol under argon. Cyclopentadiene (1.9 mL, 23.1 mmol, 2.6 equiv) and pyrrolidine (4.1 mL, 45.3 mmol, 5.1 equiv) were added, and the solution was stirred. After 19 h the dark brown solution was quenched with 2.9 mL of acetic acid (50.7 mmol, 5.7 equiv) and then 10 mL each of water and saturated aqueous NaCl. The brown mixture was extracted with 4 × 20 mL of ether. The organic extracts were combined, dried ($MgSO_4$), and filtered. The filtrate was rotoevaporated and chromatographed (3:2 hexanes: ethyl acetate), providing 0.429 g (28%) of an orange oil: ^{1}H NMR δ 8.61 (dd, J = 4.4, 1.7 Hz, 2H), 7.22 (dd, J = 4.4, 1.7 Hz, 2H), 6.58 (m, 2H), 6.47 (dm, J = 5.6 Hz, 1H), 6.08 (dt, J = 5.3, 1.7 Hz, 1H), 2.46 (s, 3H); ^{13}C NMR δ 149.01, 148.95, 145.10, 144.12, 132.66, 132.34, 123.11, 122.41, 120.62, 21.41; MS *m/z* ($M^{\bullet+}$) 169 (80), 168 (66), 154 (100); HRMS for $C_{12}H_{11}N$, calcd 169.0891, found 169.0882; UV (CH_2Cl_2) λ_{max} 284, 375 nm.

2,6-Pyridinediylbisfulvene (12f). From 2.82 g of 2,6-diacetylpyridine (17.28 mmol), 25 mL of methanol, 7.1 mL of cyclopentadiene (86.15 mmol, 2.5 equiv/equiv of ketone), and 4.4 mL of pyrrolidine (48.62 mmol, 1.4 equiv/equiv of ketone), stirred for 20 h, was obtained an orange-brown mixture. This was suction filtered (paper), providing an orange-brown powder which became lighter orange on rinsing with cold methanol. The powder was dried, providing 2.44 g (54%) of bisfulvene. The mother liquor from the filtration was chromatographed (5−15% ethyl acetate in hexanes), affording an additional 0.66 of g bisfulvene (total 3.10 g, 69%): ^{1}H NMR δ 7.75 (t, J = 7.8 Hz, 1H), 7.40 (d, J = 7.8 Hz, 2H), 6.68 (m, 2H), 6.59 (m, 2H), 6.52 (m, 2H), 6.34 (m, 2H), 2.64 (s, 6H); ^{13}C NMR δ 158.59, 147.70, 144.49, 135.44, 132.36, 124.43, 123.17, 121.82, 20.87; MS *m/z* ($M^{\bullet+}$) 259 (82), 258 (72), 244 (100); HRMS for $C_{19}H_{17}N$, calcd 259.1361, found 259.1357.

3,5-Pyridinediylbisfulvene 10f. From 1.38 g of 3,5-diacetylpyridine (**10k**) (8.46 mmol), 12 mL of methanol, 3.5 mL of cyclopentadiene (42.5 mmol, 2.5 equiv/equiv of ketone), and 4.4 mL of pyrrolidine (48.6 mmol, 2.9 equiv/equiv of ketone), stirred for 24 h, was obtained a dark brown oil. This was rotoevaporated and chromatographed (4:1 hexanes−ethyl acetate), providing 0.310 g (14%) of bisfulvene. Preparation with CpMgBr gave a 6% yield: ^{1}H NMR δ 8.62 (d, J = 2.2 Hz, 2H), 7.70 (t, J = 2.2 Hz, 1H), 6.7−6.6 (m, 2H), 6.54 (br d, J = 5.4 Hz, 1H), 6.13 (dt, J = 5.1, 1.7 Hz, 1H), 2.58 (s, 6H); MS *m/z* ($M^{\bullet+}$) 259 (72), 258 (79), 244 (100); HRMS for $C_{19}H_{17}N$, calcd 259.1361, found 259.1358; UV (CH_2Cl_2) λ_{max} 298, ∼381 (sh) nm.

(29) Micheel, F.; Dralle, H. *Justus Liebigs Ann. Chem.* **1963**, *670*, 57−68.

(30) Skala, V.; Kuthan, J.; Dedina, J.; Schraml, J. *Collect. Czech. Chem. Commun.* **1974**, *39*, 834−841.

(31) Queguiner, G.; Pastour, P. *Bull. Soc. Chim. Fr.* **1969**, *11*, 4082−4086.

2,4-Pyridinediylbisfulvene 11f. From 1.00 g of 2,4-diacetylpyridine (6.13 mmol), 13 mL of methanol, 2.6 mL of cyclopentadiene (31.5 mmol, 2.6 equiv/equiv of ketone), and 5.6 mL of pyrrolidine (61.9 mmol, 5.1 equiv/equiv of ketone), stirred for 17 h, was obtained a dark brown solution. This was quenched with 3.9 mL of acetic acid (68.1 mmol, 5.6 equiv/equiv of ketone) and rotoevaporated to remove methanol. The residue was treated with 10 mL each of water and saturated aqueous NaCl and then extracted with 6 × 20 mL of ether. The ether extracts were combined, dried ($MgSO_4$), and filtered. The filtrate was rotoevaporated and chromatographed (8:1 hexanes−ethyl acetate), affording 0.205 g (13%) of an orange oil. Preparation with CpMgBr gave only a trace of bisfulvene: ^{1}H NMR δ 8.67 (dd, J = 5.0, 0.6 Hz, 1H), 7.38 (dd, J = 1.7, 0.6 Hz, 1H), 7.21 (dd, J = 5.0, 1.7 Hz, 1H), 6.65 (dt, J = 5.3, 1.6 Hz, 1H), 6.58 (m, 3H), 6.49 (dm, J = 5.3 Hz, 2H), 6.27 (dt, J = 5.3, 1.7 Hz, 1H), 6.12 (dt, J = 5.3, 1.7 Hz, 1H), 2.63 (s, 3H), 2.50 (s, 3H); ^{13}C NMR δ 158.89, 149.21, 148.70, 147.00, 145.10, 144.47, 144.43, 132.99, 132.71, 132.44, 132.35, 124.81, 122.73, 122.57, 122.50, 121.56, 120.84, 21.74, 20.72; MS *m/z* ($M^{\bullet+}$) 259 (100), 244 (75); HRMS for $[M-H]^+$ $C_{19}H_{16}N$, calcd 258.1283, found 258.1297; UV (CH_2Cl_2) λ_{max} 292 nm.

Preparation of Carbamates by DMAD Addition to Fulvenes: 2-Pyridinecarbamate 18r. Fulvene **18f** (0.631 g, 3.73 mmol) was dissolved in 20 mL of CH_2Cl_2 under argon. DMAD (0.607 g, 4.15 mmol, 1.11 equiv) in 5 mL of CH_2Cl_2 was added. After 2 h, the solution was cooled in an ice−water bath and 2.17 g of PADC (11.2 mmol, 3.0 equiv) was added. A solution of 1.57 mL of acetic acid (27.4 mmol, 7.3 equiv) in 3 mL of CH_2Cl_2 was added dropwise over 20 min. The mixture was stirred overnight as the ice bath melted. The mixture was quenched with 20 mL of water, and the layers were shaken and separated. The aqueous layer was extracted with 25 mL of CH_2Cl_2. The organic extracts were combined, dried (K_2CO_3), and filtered. The filtrate was rotoevaporated and chromatographed (2:1 hexanes−ethyl acetate), providing 0.914 g of a brown foam. In this case, ^{1}H NMR indicated incomplete reduction, so the material was resubjected to the reduction conditions above, and the filtrate was rotoevaporated to provide 0.856 g (72%) of a foamy brown solid: ^{1}H NMR δ 8.59 (dd, J = 4.8, 0.6 Hz, 1H), 7.69 (dd, J = 7.6, 1.3 Hz, 1H), 7.29 (br s, 1H), 7.20 (ddd, J = 7.6, 4.8, 0.6 Hz, 1H), 5.06 (br m, 2H), 3.79 (br m, 6H), 2.19 (s, 3H), 1.98 (br m, 4H); ^{13}C NMR δ 158.05, 157.3 (w br), 148.81, 137.68, 136.05, 123.90, 122.10, 121.95, 59.31 (br m), 53.23, 52.96, 27.8 (br m), 26.5 (br m), 18.29; MS *m/z* ($M^{\bullet+}$) 317 (8), 171 (70), 170 (100); HRMS for $C_{16}H_{19}N_3O_4$, calcd 317.1376, found 317.1362.

3-Pyridinecarbamate 16r. From 0.414 g of fulvene **16f** as above, chromatographed using 1:2 hexanes−ethyl acetate, was isolated 0.601 g (77%) of a sticky slightly foamy pale yellow solid: ^{1}H NMR δ 8.55 (d, J = 4.7 Hz, 1H), 8.48 (s, 1H), 7.60 (d, J = 7.7 Hz, 1H), 7.34 (dd, J = 7.7, 4.7 Hz, 1H), 5.07−4.57 (br m, 2H), 3.81 (s, 3H), 3.74 (s, 3H), 2.15 (s, 3H), 1.93 (br m, 4H); ^{13}C NMR δ 158.2, 156.9, 147.86, 147.55, 136.80, 136.16, 134.62, 122.84, 121.32, 58.83, 52.78, 26.46 (br m), 19.58 (br); MS *m/z* ($M^{\bullet+}$) 317 (65), 230 (54), 171 (55), 170 (100); HRMS for $C_{16}H_{19}N_3O_4$, calcd 317.1376, found 317.1378.

4-Pyridinecarbamate 17r. From 0.424 g of fulvene **17f** as above, chromatographed using ethyl acetate, was isolated 0.752 g (94%) of a foamy off-white solid: ^{1}H NMR δ 8.60 (d, J = 4.8 Hz, 2H), 7.16 (d, J = 4.8 Hz, 2H), 5.06−4.59 (br m, 2H), 3.82 (s, 3H), 3.74 (s, 3H), 2.12 (s, 3H), 2.2−1.58 (br m, 4H); ^{13}C NMR δ 149.33, 148.77, 137.62, 122.66, 122.34, 59.12 (br), 53.30 (br) 26.7 (br m), 19.61 (br); MS *m/z* ($M^{\bullet+}$) 317 (93), 289 (52), 230 (99), 186 (56), 170 (100), 49 (46); HRMS for $C_{16}H_{19}N_3O_4$, calcd 317.1376, found 317.1380.

2,6-Pyridinebiscarbamate 12r. From 0.396 g of bisfulvene **12f**, chromatographed using 1:2 hexanes−ethyl acetate, was isolated 0.623 g (73%) of a foamy yellow-brown solid: ^{1}H NMR δ 7.69 (br t, J = 7.7 Hz, 1H), 7.21 (br s, 2H), 5.07 (br m, 4H), 3.80 (br s, 6H), 3.75 (br s, 6H), 2.20 (2s, $\Delta\delta$ = 1.8 Hz, tot 6H), 1.98 (br m, 8H); ^{13}C NMR δ 157.50 (m), 137.95, 136.70, 124.10, 120.98 (br), 59.62 (br), 53.24 (m), 26.56 (br m), 18.54 (br); DEI-MS *m/z* ($M^{\bullet+}$) 555 (18), 409 (63), 321 (18), 262 (38), 261 (21), 260 (28), 59 (100); HRMS for $C_{27}H_{33}N_5O_8$, calcd 555.2329, found 555.2318.

3,5-Pyridinebiscarbamate 10r. Bisfulvene **10f** (0.310 g, 1.20 mmol) was dissolved in 10 mL of CH_2Cl_2 under argon. DMAD (0.430 g, 2.90 mmol, 1.2 equiv/equiv of fulvene) in 5 mL of CH_2Cl_2 was added. After 30 min, another 0.43 g of DMAD was added. After 30 min, the solution was rotoevaporated, and the residue was chromatographed (1:5 hexanes−ethyl acetate), providing 0.466 g (70%) of the unreduced bis-adduct **10u** as a foamy yellow solid: ^{1}H NMR δ 8.30 (dd, J = 6.5, 2.1 Hz, 2H), 7.33 (br s, 1H), 6.80 (br s, 4H), 5.9−5.0 (br m, 4H), 3.81 (s, 6H), 3.74 (s, 6H), 2.06 (s, 6H). A 0.453 g portion of **10u** was reduced as described above, providing 0.436 g (96%; 67% for two steps) of **10r** as a foamy yellow solid: ^{1}H NMR δ 8.36 (dd, J = 7.1, 2.0 Hz, 2H), 7.41 (br s, 1H), 5.2−4.5 (br m, 4H), 3.86 (s, 6H), 3.74 (s. 6H), 2.14 (s, 6H), 2.2−1.7 (2 br s, 8H); ^{13}C NMR δ 157 (br), 147.36, 137.64, 136.22, 133.59, 121.44, 59.4, 53.4 (br) 27.3 (v br), 20.3 (br); FAB-MS *m/z* (MH^+) 556. HRMS for ($[M + H]^+$) $C_{27}H_{34}N_5O_8$, calcd 556.2407, found 556.2388.

2,4-Pyridinebiscarbamate 11r. From 0.200 g of bisfulvene **11f**, chromatographed using 1:2 hexanes−ethyl acetate, was isolated 0.263 g (61%) of a foamy pale yellow-orange solid: ^{1}H NMR δ 8.58 (d, J = 5.1 Hz, 1H), 7.04 (br m, 2H), 5.21−4.48 (br m, 4H), 3.82 (s, 6H), 3.75 (s, 6H), 2.20 and 2.14 and 2.07 (each s, tot 6H), 1.98 (br m, 8H); ^{13}C NMR δ 158.48, 157.42, 149.06, 148.78, 138.36, 137.65, 123.64, 122.80, 120.99, 120.84, 59.37, 53.33, 26.57, 20.8, 19.7, 18.6; DEI-MS *m/z* ($M^{\bullet+}$) 555 (33), 409 (100), 408 (45); HRMS for $C_{27}H_{33}N_5O_8$, calcd 555.2329, found 555.2328.

Representative Preparation of Diazenes: 2-Pyridinediazene 18-(N_2). Carbamate **18r** (0.225 g, 0.747 mmol) and powdered 87% KOH (686 mg, 15 equiv) were degassed three times on the vacuum line and purged for 10 min with argon. Isopropyl alcohol (20 mL, degassed by 30 min of argon bubbling) was added via cannula, and the mixture was stirred and heated to reflux for 90 min. The light brown mixture was cooled to room temperature, and 0.89 g of $NaHCO_3$ (15 equiv) was added. The mixture was stirred for 1 h at room temperature, and the solvent was pumped off overnight. The light brown residue was partitioned between 25 mL each of water and CH_2Cl_2 with gentle shaking, and the layers were separated. The aqueous layer was extracted with 25 mL of CH_2Cl_2. The organic layers were combined, dried (K_2CO_3), filtered, and cooled in an ice−water bath. Nickel peroxide (NiO_x, 1.21 g) was added, and the mixture was stirred in the dark. After 1 h the mixture was filtered through Celite and rotoevaporated, providing 111 mg (75%) of a pale yellow film, dried while being cooled in an ice−water bath: ^{1}H NMR δ 8.54 (d, J = 4.8 Hz, 1H), 8.40 (s, 1H), 7.47 (d, J = 7.9 Hz, 1H), 7.29 (dd, J = 7.9, 4.8 Hz, 1H), 5.53 (s, 1H), 5.23 (s, 1H), 2.03 (s, 3H), 1.79 (m, 2H), 1.20 (m, 2H); ^{13}C NMR δ 148.23, 148.07, 143.26, 135.86, 134.29, 122.79, 121.28, 74.03, 73.94, 21.05, 20.79, 19.32; UV (CH_2Cl_2) λ_{max} ∼266 (sh), 330, 338 nm.

3-Pyridinediazene 16(N_2). From 0.222 g of carbamate **16r** was isolated 104 mg (75%) of an off-white solid: ^{1}H NMR δ 8.58 (dm, J = 4.8 Hz, 1H), 7.66 (td, J = 7.7, 1.8 Hz, 1H), 7.17 (m, 2H), 5.63 (d, J = 2.4 Hz, 1H), 5.53 (d, J = 2.4 Hz, 1H), 2.08 (s, 3H), 1.82 (m, 2H), 1.18 (m, 2H); ^{13}C NMR δ 157.76, 148.79, 144.66, 135.90, 123.66, 121.90, 121.79, 74.53, 74.18, 21.00, 20.73, 17.83; UV (CH_2Cl_2) λ_{max} 270, 332, 338 nm.

4-Pyridinediazene 17(N_2). From 0.250 g of carbamate **17r** was isolated 89 mg (57%) of a pale yellow oil: ^{1}H NMR δ 8.58 (d, J = 6.0 Hz, 2H), 7.05 (d, J = 6.0 Hz, 2H), 5.52 (d, J = 2.2 Hz, 1H), 5.26 (d, J = 2.2 Hz, 1H), 2.02 (s, 3H), 1.79 (m, 2H), 1.19 (m, 2H); ^{13}C NMR δ 149.57, 147.97, 144.03, 122.43, 122.06, 74.12, 73.94, 21.04, 20.80, 18.89; UV (CH_2Cl_2) λ_{max} 338 (sh) nm.

2,6-Pyridinebisdiazene 12(N_2)$_2$. From 0.272 g of biscarbamate **12r** was isolated a pale yellow film, which was chromatographed (2:3 hexanes−ethyl acetate), providing a pale yellow film: ^{1}H NMR (300 MHz) δ 7.66 (t, J = 7.8 Hz, 1H), 7.07 (dd, J = 7.8 Hz, $\Delta\delta$ = 1.5 Hz), 5.65 (d, J = 2.19 Hz) and 5.62 (d, J = 2.21 Hz) and 5.55 (d, J = 2.24 Hz) (∼1:1:2, tot 4H), 2.12 (d, $\Delta\delta$ = 1.38 Hz, 6H), 1.85 (m, 4H), 1.21 (m, 4H). The peaks between 5.65 and 5.55 ppm show further fine splitting with J ∼ 0.6 Hz. The separation between the 5.65 and 5.62 ppm peaks is 10.3 Hz. ^{1}H NMR (400 MHz) δ 7.63 (t, J = 7.8 Hz, 1H), 7.04 (dd, J = 7.8 Hz, $\Delta\delta$ = 2.3 Hz), 5.65 (d, J = 2.34 Hz) and 5.62 (d, J = 2.32 Hz) and 5.55 (d, J = 2.32 Hz) (∼1:1:2, tot 4H), 2.08 (d, $\Delta\delta$ = 2.0 Hz, 6H), 1.85 (m, 4H), 1.22 (m, 4H). The peaks between 5.65 and 5.55 ppm show further fine splitting with J∼0.6 Hz. The separation between the 5.65 and 5.62 ppm peaks is 14.2 Hz. Decoupling experiments were performed. Irradiating the 1.85 ppm peak

converts the 5.65−5.55 ppm peaks into singlets. Irradiating the 1.22 ppm peak removes only the ∼0.6 Hz extrafine splittings of these peaks. ^{13}C NMR δ 158.84, 158.78, 146.54, 146.34, 137.57, 137.55, 124.90, 124.70, 121.50, 121.40, 74.86, 74.42, 74.36, 20.25, 20.17, 19.98, 19.90, 16.98, 16.94; UV (CH_2Cl_2) λ_{max} 286, 338 nm. The ∼1:1 integrations for the pyridine ring, bridgehead, and methyl hydrogen peaks in the ^{1}H NMR spectra indicate a ∼1:1 mixture of *syn* and *anti* isomers of the bisdiazene.

3,5-Pyridinebisdiazene 10(N$_2$)$_2$. From 0.104 g of biscarbamate **10r** was isolated a pale yellow film, which was chromatographed (ethyl acetate), providing a white solid: ^{1}H NMR δ 8.30 (m, 2H), 7.21 (m, 1H), 5.54 (m, 2H), 5.22 (m, 2H), 2.04 (2s, $\Delta\delta$ = 3.0 Hz, 6H tot), 1.91−1.71 (m, 4H), 1.34−1.12 (m, 4H); ^{13}C NMR δ 147.30, 144.13, 144.10, 135.89, 135.86, 133.25, 133.18, 121.21, 74.40, 74.34, 74.29, 21.45 (br), 21.09, 19.73; UV (CH_2Cl_2) λ_{max} 279, 332, 338 nm. The ∼1:1 integrations for the methyl hydrogen peaks in the ^{1}H NMR spectrum indicate a ∼1:1 mixture of *syn* and *anti* isomers of the bisdiazene.

2,4-Pyridinebisdiazene 11(N$_2$)$_2$. From 0.258 g of biscarbamate **11r** was isolated a pale yellow film, which was chromatographed (1:6 hexanes−ethyl acetate), providing 76 mg (51%) of a white solid: ^{1}H NMR δ 8.56 (d, J = 5.2 Hz, 1H), 6.93 (dd, J = 5.2, 2.0 Hz, 1H), 6.89 (m, 1H), 5.63 (dd, J = 4.3, 1.8 Hz, 1H), 5.53 (dd, J = 5.7, 1.8 Hz, 2H), 5.26 (m, 1H), 2.10, 2.09, 2.03, 2.02 (each s, tot 6H), 1.83 (m, 4H), 1.22 (m, 4H); ^{13}C NMR δ 158.24, 158.20, 148.56, 148.53, 145.30, 144.25, 144.23, 123.52, 122.57, 120.73, 120.67, 120.55, 120.50, 74.71, 74.40, 74.36, 74.24, 74.14, 74.08, 21.22, 21.19, 21.12, 20.92, 19.15, 18.07; UV (CH_2Cl_2) λ_{max} 276 (sh), 338 (sh) nm. The ∼1:1 integrations for the two pairs of methyl hydrogen peaks in the ^{1}H NMR spectrum indicate a ∼1:1 mixture of *syn* and *anti* isomers of the bisdiazene.

Consecutive NMR and EPR Spectra of Pyridine-Ring-Protonated Diazenes 18(N$_2$) and 19(N$_2$). Separate solutions of **18(N$_2$)** and **19-(N$_2$)** were prepared, ∼20 mM in EtOH-d_6. ^{1}H NMR spectra were recorded, then 1 drop of CF_3CO_2D or several milligrams of TsOH·H_2O was added, and the spectra were re-recorded. Note that NMR peaks of EtOH-d_6 at ∼5.5, 3.5, and 1.1 ppm obscure portions of the re-recorded spectra. Peaks due to TsOH were observed at 7.70 (d), 7.19 (d), and 2.35 (s) ppm.

2-Pyridinediazene 18(N$_2$). Before adding the acid source: ^{1}H NMR δ 8.54 (dm, J = 4.8 Hz, 1H), 7.80 (td, J = 7.8, 1.8 Hz, 1H), 7.28 (m, 2H), 5.59 (d, J = 2.6 Hz, 1H), 5.49 (d, J = 2.6 Hz, 1H), 2.08 (s, 3H), 1.87 (m, 2H). Treated with TsOH: ^{1}H NMR δ 8.85 (dm, J = 5.9 Hz, 1H), 8.64 (td, J = 8.0, 1.6 Hz, 1H), 8.04 (t, J = 7.0 Hz, 1H), 7.93 (d, J = 8.0 Hz, 1H), 5.63 (d, J = 2.3 Hz, 1H), 5.19 (d, J = 2.3 Hz, 1H), 2.19 (s, 3H), 1.90 (m, 2H). From relative integrals the mole ratio of diazene to TsOH was ∼4.7:1.0. Treated with CF_3CO_2D: ^{1}H NMR δ 8.78 (dd, J = 5.5, 1.2 Hz, 1H), 8.45 (td, J = 7.8, 1.2 Hz, 1H), 7.88 (ddd, J = 7.8, 5.5, 1.2 Hz, 1H), 7.78 (d, J = 7.8 Hz, 1H), 5.64 (d, J = 2.6 Hz, 1H), 5.25 (d, J = 2.6 Hz, 1H), 2.17 (s, 3H), 1.91 (m, 2H).

3-Pyridinediazene 16(N$_2$). Before adding the acid source: ^{1}H NMR δ 8.47 (dm, J = 4.8 Hz, 1H), 8.34 (s, 1H), 7.67 (dm, J = 7.9 Hz, 1H), 7.44 (dd, J = 7.9, 4.8 Hz, 1H), 5.60 (s, 1H), 5.13 (d, J = 1.7 Hz, 1H), 2.06 (s, 3H), 1.85 (m, 2H). Treated with TsOH: ^{1}H NMR δ 8.85 (dd, J = 5.8, 0.8 Hz, 1H), 8.79 (m, 1H), 8.50 (dt, J = 8.1, 1.7 Hz, 1H), 8.13 (dd, J = 8.2, 5.8 Hz, 1H), 5.62 (d, J = 2.1 Hz, 1H), 5.22 (d, J = 2.1 Hz, 1H), 2.13 (s, 3H), 1.93 (m, 2H). From relative integrals the mole ratio of diazene to TsOH was ∼7.4:1.0. Treated with CF_3CO_2D: ^{1}H NMR δ 8.82 (d, J = 5.5 Hz, 1H), 8.75 (m, 1H), 8.41 (dm, J = 7.6 Hz, 1H), 8.05 (dd, J = 7.6, 5.5 Hz, 1H), 5.64 (d, J = 2.5 Hz, 1H), 5.21 (d, J = 2.5 Hz, 1H), 2.14 (s, 3H), 1.91 (m, 2H).

The samples of **18(N$_2$)** and **16(N$_2$)** after acid treatment were immediately degassed, frozen, and photolyzed without dilution. EPR spectra were the same as those in Figure 10 from conventionally prepared EPR samples.

NMR Spectra of Pyridine-Ring-Protonated Bisdiazenes 12(N$_2$)$_2$ and 10(N$_2$)$_2$. 2,6-Pyridinebisdiazene 12(N$_2$)$_2$. Before adding acid source: ^{1}H NMR δ 7.79 (t, J = 7.8 Hz, 1H), 7.19 (dd, J = 7.8, 3.0 Hz, 2H), 5.63 (s, J = 1.8 Hz, 1H), 5.61 (s, J = 1.8 Hz, 1H), 2.12 (d, $\Delta\delta$ = 2.1 Hz, 6H), 1.89 (m, 4H). Bubbled with HCl(g): ^{1}H NMR δ 8.65 (m, 1H), 7.84 (dm, J = 6.9 Hz, 2H), 5.64 (s, 2H), 5.20 (s, 2H), 2.23 (s, 6H), 2.02 (br m, 4H). Treated with TsOH: ^{1}H NMR δ 8.52 (dt, $\Delta\delta$ = 5.5 Hz, J = 8.0 Hz, 1H), 7.74 (dd, $\Delta\delta$ = 3.4 Hz, J = 8.0 Hz, 2H), 5.60 (m, 2H), 5.20 (m, 2H), 2.18 (d, $\Delta\delta$ = 2.1 Hz, 6H), 1.96 (m, 4H). From relative integrals the mole ratio of diazene to TsOH was ∼10.2:1.0.

3,5-Pyridinebisdiazene 10(N$_2$)$_2$. Before adding the acid source: ^{1}H NMR δ 8.28 (s, 2H), 7.44 (t, J = 2.1 Hz, 1H), 5.61 (s, 2H), 5.15 (s, 2H), 2.08 (d, $\Delta\delta$ = 1.5 Hz, 6H), 1.86 (d, J = 6.0 Hz, 4H). Treated with TsOH: ^{1}H NMR δ 8.69 (s, 2H), 8.25 (s, 1H), 5.62 (s, 2H), 5.26 (s, 2H), 2.14 (s, 6H), 1.93 (m, 4H). From relative integrals the mole ratio of diazene to TsOH was ∼6.9:1.0.

Samples of **12(N$_2$)$_2$** and **10(N$_2$)$_2$** at concentrations suitable for NMR were too concentrated to allow a significant extent of photolysis for the EPR experiments.

Description of Kinetics Experiments (Figure 14). Samples were prepared in pairs, each pair consisting of one sample of **15(N$_2$)$_2$** (TFA or tosylate counterion, ∼0.3 mM bisdiazene) and one of **12(N$_2$)$_2$**, **17-(N$_2$)$_2$**, or **21(N$_2$)** (∼0.3 mM bisdiazene or ∼0.6 mM monodiazene). The members of each pair were photolyzed in either order at 77 K on the same day. The Δm_s = 1 double-integral signal intensities were determined as a function of photolysis time and plotted in Figure 14. The Δm_s = 2 peak−peak intensities gave qualitatively similar plots.

Acknowledgment. We thank Professor W. A. Goddard for helpful discussions, and the Molecular Simulations Center of the Beckman Institute at Caltech. This work was supported by the National Science Foundation. A.P.W. and S.K.S. thank the NSF for predoctoral fellowships.

Supporting Information Available: Tables of UHF and GVB geometries of structures **1** and **3**−**8** (8 pages). This material is contained in libraries on microfiche, immediately follows this article in the microfilm version of the journal, can be ordered from the ACS, and can be downloaded from the Internet; see any current masthead page for ordering information and Internet access instructions.

JA9527941